J Math Chem (2014) 52:741–753
DOI 10.1007/s10910-013-0292-y

ORIGINAL PAPER

A model of cooperativity based on restricted binding: kinetic and thermodynamic analysis

Kinshuk Banerjee

Received: 4 October 2013 / Accepted: 7 November 2013 / Published online: 16 November 2013

Abstract Cooperative protein–ligand binding is an essential biochemical process. In this work, we introduce a model that can simulate the emergence of such phenomenon in the binding kinetics. It is based on the inability of the ligand molecules to fully utilize all the available binding sites due to some restriction, realized here in terms of a model parameter, called the restriction parameter. The theory is developed at the level of a single oligomeric protein molecule interacting with a ligand, maintained at a constant concentration, using a chemical master equation. The model provides stepwise binding constants related to the restriction parameter. The relative magnitudes of these constants, when compared to the Hill coefficients measuring cooperativity, give a physical insight in the development of the cooperative behavior and can also act as a reference frame. This can be useful for an alternative theoretical characterization of cooperativity in oligomeric proteins with large number of binding sites and arbitrary binding constants. We establish this point here by taking a tetrameric protein as a case study. A stochastic thermodynamic analysis is also performed, highlighting the energy–entropy contribution to the overall free energy change due to protein–ligand interaction for various cases of restricted binding.

Keywords Oligomeric protein · Cooperativity · Master equation · Stochastic thermodynamics

1 Introduction

Oligomeric proteins are quite ubiquitous in nature [1–3], most famous being the haemoglobin molecule involved in oxygen binding [4,5]. The multiple sites of these

K. Banerjee (✉)
Department of Chemistry, University of Calcutta, Kolkata 700009, India
e-mail: banerjee.kinshuk8@gmail.com

proteins for ligand binding can be independent or interacting. An example of the former case is the *Escherichia coli* β-galactosidase enzyme which is tetrameric with non-interacting sub-units [6]. The latter case is more interesting as interaction among the sub-units can give rise to cooperativity in protein–ligand binding which is a very important biological process [7–11]. There are various examples of cooperative behavior, again a prime contender being haemoglobin that shows sigmoidal oxygen binding curve [7]. This is a signature of positive cooperativity where the binding of one ligand molecule with a subunit increases the affinity of further attachment of the ligand to other subunits [8,11]. Similarly, in negative cooperativity, attachment of a ligand molecule to one subunit reduces the tendency of further attachment of the ligand to other subunits [12,13]. Generally, these types of cooperativity are classified under allosteric cooperativity [9]. The phenomena are well-studied in literature with the kinetics being theoretically analyzed in terms of two well established models: the Monod–Wyman–Changeux (MWC) model [14] and the Koshland–Nemethy–Filmer (KNF) model [15]. The KNF model is based on sequential binding of ligands to the multimeric protein with site-dependent binding constants. On the other hand, MWC model is formulated in terms of different conformations of the protein having different affinities for the ligand [9]. These schemes for allosteric cooperativity are necessarily applicable to multimeric proteins. Now, advent of modern experimental techniques, particularly single molecule spectroscopy [16–18], allows one to probe various binding and catalytic processes with much greater detail. As a consequence, interest has been rekindled in relevant theoretical studies. Stochastic kinetics at the mesoscopic scale [19–22] received a lot of attention in this regard. This is due to the fact that, the theory at the single molecule level must be constructed in terms of the probabilities of possible system states, instead of concentrations of species, as in bulk reaction [23,24]. For example, the ligand-binding kinetics of a single oligomeric protein is described in terms of the probabilities of its ligand-bound states, with number of ligands bound at any instant of time being a stochastic or random variable [25–27]. The kinetics is formulated in terms of a master equation, aptly called chemical master equation [28].

In this paper, we introduce a model of cooperativity, called the restricted binding model, which is basically a generalization of the sequential binding mechanism. The restriction imposed is: *not all the sites are available for binding and this availability varies during the successive binding steps.* This gives rise to cooperativity in the ligand binding, which can be described using the standard Hill coefficient measure. The utility of our model can be best understood by comparing it with the standard sequential binding model. In the latter case, cooperativity is generated when the successive ligand-binding steps have different binding constants. For a dimeric protein, the nature of cooperativity can be trivially found for this scheme. But, the situation gets gradually more complicated with increasing number of binding sites. Then, one has no option but to characterize the cooperativity for each case separately. With intractable number of possible combinations of binding constants in principle, this is a futile task. Of course, for gradually rising or falling binding constant values or when one of the binding constants is hugely different from the others, the cooperativity can be described. However, for a coherent theoretical understanding of cooperativity based on such a mechanism, one faces the basic question: what is the reference frame to judge the case

of arbitrary stepwise binding constants in governing the nature and extent of cooperativity? We show here that, the restricted binding model provides such a reference frame of site-dependent binding constants, taking a single tetrameric protein as an example.

There has been extensive research in the field of thermodynamics of small systems, focusing specially on situations far away from equilibrium [29–37]. Formulation of thermodynamics at the single trajectory level in the past few years have allowed the general thermodynamic concepts to be applicable for such systems [38–40]. Here we implement this methodology to describe also the thermodynamics of stochastic protein–ligand binding, complementing the kinetics.

In what follows, we construct the master equation for the restricted ligand binding scheme in Sect. 2, along with the steady state solution. In Sect. 3, the state function quantities, like internal energy, entropy and free energy of the system are introduced based on the stochastic thermodynamic methodology and thoroughly analyzed for various binding mechanisms. The nature of cooperativity in the restricted binding kinetics and the corresponding thermodynamics are discussed in Sect. 4, concentrating on the energy–entropy contribution to the free energy change. The paper is concluded in Sect. 5.

2 Master equation for restricted binding and cooperativity

We take an oligomeric protein consisting of n_T number of sub-units. Each sub-unit can bind a single ligand molecule. We start with the condition of a fully vacant protein at time, $t = 0$. For independent binding of the ligand in the normal case, all the n_T sub-units will be available for the first ligand molecule to bind. But for the restricted binding model studied here, the number of available sub-units can also be less than n_T. This is for the first step of the binding. For the subsequent attachments, the restrictions can be applied similarly. Generally, the master equation for this restricted binding scheme is written as

$$\begin{aligned}\frac{\partial P(n,t)}{\partial t} &= k_1(n_T - r_{n-1})P(n-1,t) + (n+1)k_2P(n+1,t) \\ &\quad - k_1(n_T - r_n)P(n,t) - nk_2P(n,t). \end{aligned} \tag{1}$$

The definitions of the quantities in Eq. (1) are as follows. First of all, $P(n,t)$ is the probability to find the protein molecule bound with n number of ligand molecules at time t where $n = 0, 1, \ldots, n_T$. The rate constants for the attachment and detachment of the ligand are denoted k_1, k_2, respectively. In our scheme, they are taken to be the same for all the steps. Actually, k_1 is the pseudo-first order rate constant defined as $k_1 = k_1'[L]$ where k_1' is the true second order rate constant for protein–ligand association and $[L]$ is the ligand concentration, assumed fixed for simplicity. We introduce a restriction parameter, r_n, an integer, for the attachment of a ligand molecule with the state of the protein having n number of ligand molecules already bound. There is no restriction in the detachment of the ligands from the protein–ligand complex in any step. Then it is clear that, in principle, we can take

$$r_n = n, n+1, \ldots, n_T - 1, \quad \text{for } n = 0, 1, \ldots, (n_T - 2)$$
$$r_{n_T-1} = n_T - 1, \quad r_{n_T} = n_T. \tag{2}$$

So with $r_n = n \ \forall n$, the binding process is totally unrestricted.

2.1 The steady state solution

At the steady state, the master equation (1) satisfies the detailed balance condition and hence, the system reaches equilibrium. The equilibrium solution of Eq. (1) is given as

$$P^e(n) \begin{cases} = \frac{\prod_{i=0}^{n-1}(n_T - r_i)}{n!} X^n P^e(0), & \text{for } \ n = 1, \ldots, m+1 \\ = \prod_{i=0}^{m} \left(\frac{n_T - r_i}{n_T - i}\right) \mathrm{C}_{n_T}^n X^n P^e(0), & \text{for } \ n = m+2, \ldots, n_T. \end{cases} \tag{3}$$

Here the index m gives the hierarchy of restriction in the ligand binding with $0 \leq m \leq (n_T - 2)$. For example, $m = 0$ means that the restriction, if any, is only in the first binding step. The maximum value $m = n_T - 2$ represents the case where there is restriction in the penultimate binding step. This may or may not include restrictions in the previous steps. The parameter $X = k_1/k_2 = k_1'[L]/k_2 = K_b[L]$ with K_b being the binding equilibrium constant. The equilibrium vacant state probability is given as

$$P^e(0) = (1 + Z_1 + Z_2)^{-1}, \tag{4}$$

with $Z_1 = \sum_{n=1}^{m+1} \frac{\prod_{i=0}^{n-1}(n_T - r_i)}{n!} X^n$ and $Z_2 = \prod_{i=0}^{m} \left(\frac{n_T - r_i}{n_T - i}\right) \sum_{n=m+2}^{n_T} \mathrm{C}_{n_T}^n X^n$. For unrestricted binding with $r_n = n \, \forall n$, the distribution becomes binomial as

$$P_{\text{bino}}^e(n) = \mathrm{C}_{n_T}^n \frac{X^n}{(1+X)^{n_T}}. \tag{5}$$

This is expected for independent binding of ligands without any restrictions.

2.2 Hill criteria of cooperativity

The cooperativity in ligand binding kinetics is traditionally quantified in terms of the Hill coefficient, n_H [41]. It is generally defined as the slope of the Hill plot, $\ln\left(\frac{\theta}{1-\theta}\right)$ versus $\ln[L]$ at the half-saturation point, $\theta = 0.5$. Here, θ is the fractional saturation of the protein given as $\theta = \langle n \rangle / n_T$. $\langle n \rangle$ is the average saturation at equilibrium defined as $\langle n \rangle = \sum_{n=0}^{n_T} n P^e(n)$. As θ is experimentally measurable, the Hill coefficient is extremely useful for the detection of cooperativity although it does not help in elucidating the detailed mechanism generally. The Hill criteria of cooperativity is given as

$$n_H \begin{cases} > 1, & \text{positive cooperativity} \\ = 1, & \text{no cooperativity} \\ < 1, & \text{negative cooperativity.} \end{cases} \tag{6}$$

The slope of the Hill plot can be written as

$$s_H = \frac{[L](d\theta/d[L])}{\theta(1-\theta)}. \tag{7}$$

It is shown in the literature that the r.h.s. of Eq. (7) can be written as the ratio of the variances of the number of ligands bound for a given distribution and the corresponding binomial distribution [5,41]. The expression is as follows

$$s_H = \frac{\langle n^2\rangle - \langle n\rangle^2}{n_T\theta(1-\theta)} = \frac{\sigma^2}{\sigma^2_{\text{bino}}}. \tag{8}$$

In our case, the variance in the numerator of Eq. (8) can be determined using the distribution in Eq. (3) whereas, the corresponding binomial is of the form given in Eq. (5). Then, the Hill coefficient, n_H is calculated by evaluating this ratio at $\theta = 0.5$. It is evident that, a binomial distribution of the binding number has a Hill coefficient of unity and thus corresponds to a non-cooperative binding. Thus, a distribution like that given in Eq. (3), can emerge from a cooperative binding kinetics.

3 Stochastic thermodynamics

Starting from the canonical distribution, the internal energy, $u(n)$ of the state n can be written in terms of the equilibrium probability, $P^e(n)$ as $u(n) = -T\ln P^e(n) + F^e$ where F^e is the equilibrium free energy of the system [42]. Here, we consider the whole reaction system to be in contact with an isothermal bath with temperature, T. The bath is taken to be an ideal one with no entropy production of its own [42,43]. The Boltzmann constant is set at $k_B = 1$ and we also set $F^e = 0$. The time-dependent internal energy, $U(t)$ of the system is given as [42]

$$U(t) = \langle u(n)\rangle = \sum_n u(n)P(n,t), \tag{9}$$

where $P(n,t)$ is the general time-dependent solution of the master equation. The entropy, S and free energy, F of the system are defined as

$$S(t) = -\sum_n P(n,t)\ln P(n,t) \tag{10}$$

and

$$F(t) = U(t) - TS(t) = T\sum_n P(n,t)\ln\left(\frac{P(n,t)}{P^e(n)}\right). \tag{11}$$

In our system of protein–ligand binding, as we take the initial condition to be $P(n, t = 0) = \delta_{n,0}$, the initial values of the three thermodynamic state functions introduced above are : $U(t = 0) = -T\ln P^e(0)$, $S(t = 0) = 0$ and $F(t = 0) = U(t = 0)$. Then the internal energy change as the system reaches equilibrium is expressed as

$$\begin{aligned}\Delta U = U^e - U(t=0) &= -T\sum_{n=0}^{n_T} P^e(n)\ln P^e(n) + T\ln P^e(0) \\ &= T\sum_{n=1}^{n_T} P^e(n)\ln\left(\frac{P^e(0)}{P^e(n)}\right), \end{aligned} \tag{12}$$

where we have used the normalization $\sum_{n=0}^{n_T} P^e(n) = 1$. Similarly, the entropy change is

$$T\Delta S = -T\sum_{n=0}^{n_T} P^e(n)\ln P^e(n). \tag{13}$$

Then, from Eqs. (12) and (13), we get the free energy change as

$$\Delta F = T\ln P^e(0). \tag{14}$$

The above result also follows directly from Eq. (11) with the free energy at equilibrium being zero. Thus, starting from a fully vacant protein, the free energy change due to ligand binding is governed here by the vacant state probability at equilibrium. We analyze it further in the next paragraph.

Let us compare the vacant state probabilities of the binomial distribution, Eq. (5) and the distribution corresponding to the restricted binding, Eq. (4). Their difference is given as

$$\begin{aligned}\frac{1}{P^e_{\text{bino}}(0)} - \frac{1}{P^e(0)} &= (1+X)^{n_T} - (1 + Z_1 + Z_2) \\ &= \left(\sum_{n=1}^{m+1} \mathrm{C}^n_{n_T} X^n - \sum_{n=1}^{m+1} \frac{\prod_{i=0}^{n-1}(n_T - r_i)}{n!} X^n\right) \\ &\quad + \left(\sum_{n=m+2}^{n_T} \mathrm{C}^n_{n_T} X^n \left(1 - \prod_{i=0}^{m}\left(\frac{n_T - r_i}{n_T - i}\right)\right)\right) \\ &= \sum_{n=1}^{m+1} \frac{X^n}{n!}\left[(n_T(n_T-1)\ldots(n_T-n-1))\right. \\ &\quad \left. -((n_T - r_0)(n_T - r_1)\ldots(n_T - r_{n-1}))\right] \\ &\quad + \left(\sum_{n=m+2}^{n_T} \mathrm{C}^n_{n_T} X^n \left(1 - \prod_{i=0}^{m}\left(\frac{n_T - r_i}{n_T - i}\right)\right)\right). \end{aligned} \tag{15}$$

It is evident from Eq. (15) that for $r_i = i,\ \forall i$, the r.h.s. becomes zero. This is expected as for unrestricted binding, the distribution reduces to a binomial. Now, restricted binding occurs for $r_i > i,\ \forall i$ and then, from Eq. (15) we get

$$\frac{1}{P^e_{\text{bino}}(0)} - \frac{1}{P^e(0)} > 0. \tag{16}$$

From Eqs. (14) and (16), we see that, *free energy change in the case of unrestricted binding is always more negative than the corresponding restricted binding cases*.

4 Kinetics and thermodynamics of restricted binding

We model the case of a tetrameric protein to apply the theoretical methodology introduced in the previous sections. With $n_T = 4$, the restriction in ligand binding can go up to $m = n_T - 2 = 2$, i.e., $r_i = i, i+1, \ldots, (n_T - 1)$ for $i = 0, 1, 2$ and $r_3 = 3, r_4 = 4$. First of all, we numerically determine the fractional saturation, θ as a function of X/K_b, the effective ligand concentration. The plot of θ is shown in Fig. 1 for the unrestricted binding along with some restricted binding cases. The unrestricted binding is most efficient as is evident from the figure.

We construct the Hill plot, $\ln\left(\frac{\theta}{1-\theta}\right)$ versus $\ln[L]$ and numerically determine the Hill coefficient, n_H for all possible scenarios of restricted binding for $n_T = 4$. The results are summarized in Table 1. It is evident from the given Hill coefficient data that restriction in ligand binding in different steps can give rise to both positive and negative cooperativity in binding. There are also cases where the system is almost non-cooperative. An important aspect is that here one can invoke site-dependent rate constants, $k_1^{(j)}(j = 0, 1, \ldots, (n_T - 1))$ for ligand attachment. They are defined in terms of the restriction parameter, r_j as

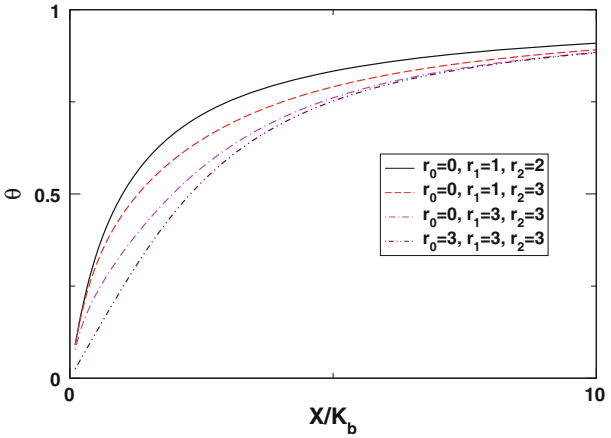

Fig. 1 The fractional saturation, θ is plotted as a function of X/K_b, the effective ligand concentration, for the unrestricted binding ($r_0 = 0,\ r_1 = 1,\ r_2 = 2$) as well as for some restricted binding cases

Table 1 All possible schemes for the restricted ligand binding to a protein with $n_T = 4$

r_0	r_1	r_2	n_H	$k_1^{(0)}:k_1^{(1)}:k_1^{(2)}:k_1^{(3)}$
0	1	2	1.0	1:1:1:1
0	2	2	1.075	1:2/3:1:1
0	3	2	1.201	1:1/3:1:1
0	1	3	0.871	1:1:1/2:1
0	2	3	0.957	1:2/3:1/2:1
0	3	3	1.11	1:1/3:1/2:1
1	1	2	1.058	3/4:1:1:1
1	2	2	1.133	3/4:2/3:1:1
1	3	2	1.258	3/4:1/3:1:1
1	1	3	0.919	3/4:1:1/2:1
1	2	3	1.007	3/4:2/3:1/2:1
1	3	3	1.157	3/4:1/3:1/2:1
2	1	2	1.154	1/2:1:1:1
2	2	2	1.228	1/2:2/3:1:1
2	3	2	1.354	1/2:1/3:1:1
2	1	3	1.0002	1/2:1:1/2:1
2	2	3	1.089	1/2:2/3:1/2:1
2	3	3	1.241	1/2:1/3:1/2:1
3	1	2	1.348	1/4:1:1:1
3	2	2	1.425	1/4:2/3:1:1
3	3	2	1.553	1/4:1/3:1:1
3	1	3	1.174	1/4:1:1/2:1
3	2	3	1.269	1/4:2/3:1/2:1
3	3	3	1.422	1/4:1/3:1/2:1

The Hill coefficient, n_H and the ratio of the effective stepwise binding rate constants, $k_1^{(j)}$ are determined for each case

$$k_1^{(j)} = k_1 \left(\frac{n_T - r_j}{n_T - j} \right). \tag{17}$$

These stepwise rate constants give the equivalent scenario of the restricted binding model described in Eq. (1). More importantly, they provide the link between the restricted binding model and the standard sequential binding mechanism and give a detailed physical insight in the development of cooperativity with stepwise different binding affinities. As already mentioned in the Introduction, it is not possible to generally determine the nature of cooperativity for arbitrary site-dependent binding constants. Hill coefficient presents a global measure without details and that also has to be implemented case-by-case. In this regard, the restricted binding scheme allows one to get some representative values of the stepwise binding constants, that reduces the arbitrariness and can throw new light on our understanding of the underlying mechanism. The ratios of the stepwise binding rate constants, $k_1^{(j)}$, given in Table 1, can serve that purpose, in conjunction with the Hill coefficient. These ratios offer a useful reference frames in judging the nature of cooperativity for an arbitrary ligand

binding case, with the following constraint. In the effective stepwise binding constants, $k_1^{(j)}$, coming out of the restricted binding model, the rate constant of the final binding step (binding of the fourth ligand molecule for $n_T = 4$) is never less than the rate constants of the previous binding steps. However, generally it can be said that, the nature of cooperativity depends on in which step the restriction is imposed, in other words, the relative magnitudes of the stepwise binding constants. This is discussed next.

Analyses of the data in Table 1 show that significant negative cooperativity can arise if the restriction comes into play at its final stage. In our case of a tetrameric protein, the lowest n_H (= 0.871) occurs for $r_0 = 0$, $r_1 = 1$, $r_2 = 3$, i.e., when restriction first appears only after binding of two ligand molecules. Following similar trend, appreciable positive cooperativity appears when the restrictions are imposed early. In our case, the maximum n_H (= 1.553) is for $r_0 = 3$, $r_1 = 3$, $r_2 = 2$, i.e., full possible restriction in the attachment of first and second ligand molecules and then no further restriction in the following steps. Also different restriction numbers, r_n, leading to different ratios of the stepwise binding constants, can conspire in such a way that the overall Hill coefficients become similar. This shows the *inability of the Hill coefficient to unveil the mechanistic details of the reaction*.

From the volume of data in Table 1, we now analyze some specific cases to see how the overall cooperativity develops. Let us take the bunch of schemes with $r_0 = 0$, $r_1 \geq 1$, $r_2 = 2$. First we discuss the variation of the restriction number r_1. For $r_1 = 2$, there is partial restriction in the attachment of the second ligand molecule to the oligomeric protein. This gives a ratio of the stepwise rate constants as $k_1^{(0)}:k_1^{(1)}:k_1^{(2)}:k_1^{(3)}::1:2/3:1:1$. Thus, although the fall of the binding constant in the second step and its rise in the third step are by the same factor (= 3/2), the rise matters more as the system is positively cooperative with $n_H = 1.075$. As the restriction becomes full with $r_1 = 3$, the fall and rise of the binding constant in the second and third step, respectively, occurs by the same factor (= 3, different from the previous case obviously). Again, the rise matters more and the system becomes more positively cooperative with $n_H = 1.201$. Thus, here the third step of ligand binding is the cooperativity determining step.

Next we come to the schemes with $r_0 = 0$, $r_1 \geq 1$, $r_2 = 3$. The restriction is full in the third binding step ($r_2 = 3$) and the restriction in the second step is gradually turned on. For $r_1 = 1$, the fall and rise of the binding constant in the third and fourth step, respectively, occurs by the same factor (=2). But now the fall matters more with the overall binding showing negative cooperativity having $n_H = 0.871$. For $r_1 = 2, 3$ the situation becomes more complex with the fall and rise of the $k_1^{(j)}$s occurring by different factors. In case of $r_1 = 2$, the binding constant in the second step falls by a factor of 3/2 and for $r_1 = 3$, it falls by a factor of 3. But the former case has negative cooperativity ($n_H = 0.957$) whereas, the latter one has positive cooperativity ($n_H = 1.11$). This shows that again the overall cooperativity is governed here by the third step of ligand attachment. For $r_1 = 2$ (with $r_0 = 0$, $r_2 = 3$), $k_1^{(2)}$ decreases compared to $k_1^{(1)}$ by a factor of 3/4 that leads to negative cooperativity. On the other hand, for $r_1 = 3$ (with $r_0 = 0$, $r_2 = 3$), it increases by a factor of 3/2 generating positive cooperativity.

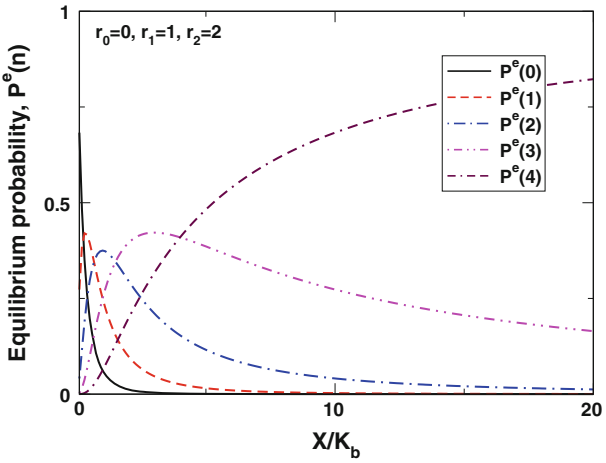

Fig. 2 The equilibrium probabilities, $P^e(n)$ are plotted as a function of X/K_b (with concentration units) for the unrestricted binding (non-cooperative) case, i.e., $r_0 = 0,\ r_1 = 1,\ r_2 = 2$

This trend gets changed when the restriction is turned on in the first step of binding itself with $r_0 > 0$. This happens particularly in the case of negative cooperativity whose occurrence becomes rarer as r_0 increases, turning the negative cases to positive ones. This transition can be characterized with the symmetric case where the ratio is $k_1^{(0)}{:}k_1^{(1)}{:}k_1^{(2)}{:}k_1^{(3)}{::}1/2{:}1{:}1/2{:}1$ for the scheme with $r_0 = 2,\ r_1 = 1,\ r_2 = 3$. Here the binding rate constants in successive steps rise and fall by the same factor $(= 2)$ that ultimately gives a system which is almost non-cooperative having $n_H = 1.0002$. When the restriction in r_0 is full with $r_0 = 3$, there is only positive cooperativity (see Table 1).

We now plot the equilibrium probabilities, $P^e(n)$ for the unrestricted binding (non-cooperative) case in Fig. 2 as a function of X/K_b. At low X/K_b, corresponding to low ligand concentration, the vacant state probability, $P^e(0)$ of the protein dominates. As X/K_b increases, $P^e(0)$ falls rapidly and the fully occupied state probability, $P^e(4)$ rises monotonically. Other state probabilities pass through maxima at intermediate ligand concentrations. This feature is present for the various restricted binding cases also (not shown in figures). The nature of variation of the equilibrium probabilities of different ligand-bound states of the protein with ligand concentration governs the thermodynamics of the stochastic binding as we will show next.

The temperature-scaled internal energy change, $\Delta U/T$ and entropy change, ΔS are shown as a function of X/K_b for the unrestricted and a few restricted binding schemes in Fig. 3. From Fig. 3a, one can see that the variation of internal energy change has two distinct regions. At small values of $X/K_b\ (\ll 1)$, $\Delta U/T$ is positive for all the binding schemes. This can be explained using Eq. (12). At low X/K_b, only the vacant state probability, $P^e(0)$ is significant, $P^e(0) \gg P^e(n),\ n \neq 0$ (see Fig. 2). Then all the terms in Eq. (12) are positive and hence $\Delta U/T > 0$. As the value of X/K_b rises, $P^e(0)$ becomes rapidly smaller than the other bound state probabilities. Thus $\Delta U/T$ becomes negative and falls continuously in the range of concentration studied. The

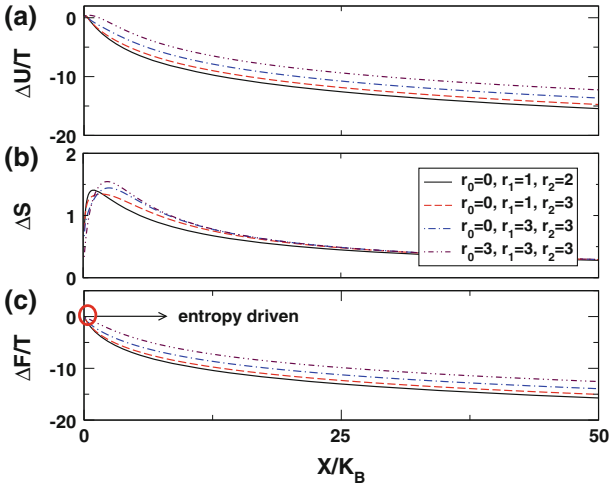

Fig. 3 Variation of **a** temperature-scaled internal energy change, $\Delta U/T$, **b** entropy change, ΔS and **c** temperature-scaled free energy change, $\Delta F/T$ due to protein–ligand binding as a function of X/K_b for the unrestricted and a few restricted binding schemes. In **c** the entropy driven binding is indicated for $X/K_b \ll 1$

variation of ΔS with X/K_b shows non-monotonic behavior as shown in Fig. 3b. In all the cases it passes through a maximum. This can again be interpreted in terms of the variation of $P^e(n)$. At the limit of $X/K_b \ll 1$, $P^e(0)$ is dominant, whereas at the other limit of $X/K_b \gg 1$, only $P^e(4)$ survives. According to Eq. (13), $\Delta S \to 0$ in both the limits. So at some intermediate X/K_b value, when some of the state probabilities will come close together having finite values (see Fig. 2), the entropy change will maximize. In this context, it is useful to point out that the uniform distribution has the maximum entropy as evident from Eq. (13).

Next, we come to the temperature-scaled free energy change, $\Delta F/T$ plotted in Fig. 3c. It is negative throughout and also decreases monotonically with ligand concentration. The free energy curve for the unrestricted binding always remains lower than those for restricted binding, supporting the analytical result derived in Eq. (16). Hence, although the restricted binding cases in our model are positively or negatively cooperative in general, their binding efficiency is lower than the unrestricted non-cooperative binding scheme. Thus, binding efficiency has no direct connection to the degree of cooperativity. We want to mention further couple of important points. (i) From the variations of internal energy, entropy and free energy, it becomes clear that the ligand binding process is internal energy driven over most of the range of ligand concentration. This is true for the non-cooperative as well as the cooperative schemes arising out of restricted binding. (ii) In connection with the first point, at very low ligand concentration, the internal energy change is positive for all the cases. So in this limit, the energy contribution is unfavorable to the overall free energy change. However, the binding process can still go on by the (positive) entropy contribution that makes the overall free energy change negative. Therefore, in the limit of low ligand concentration, the binding process is entropy driven.

5 Conclusion

In this work, we have introduced a model of cooperative ligand binding to a single oligomeric protein molecule, based on a restriction over available sites during the binding process. The stochastic kinetics is described in terms of a chemical master equation. The hierarchy of restrictions in the binding schemes can be physically realized in terms of the site-dependent binding rate constants, determined from the restriction parameter of the model. This parameter governs in which step and to what extent the restrictions are imposed on ligand attachment, generating both positive and negative cooperativity. The relative magnitudes of the stepwise binding rate constants for all possible scenarios of restricted association are analyzed by taking the case of a tetrameric protein. The ratios of the binding constants, along with the Hill coefficients, furnish a detailed understanding of the underlying machinery of cooperative binding. This is important, as the Hill coefficient alone tells nothing about the local interactions that give the resultant behavior. Thorough analyses of our data in various cases show that, when the restriction is imposed only in the second and/or third step of binding, negative cooperativity arises in several cases. With no restriction in the first binding step, the third step of ligand binding is identified as the crucial step that governs the nature of cooperativity showing the utility of the method in determining the mechanistic details, although limited by constraints of the model. With increasing restrictions in the first binding step, positive cooperativity becomes the dominant feature, with the first and second steps becoming important. This shift in the importance of the ligand binding steps in controlling the overall cooperative behavior is nicely characterized by a case of symmetric stepwise binding constants, where they cancel out the effects of each other, giving the system an overall non-cooperative nature. Therefore, the restricted binding model shows the inadequacy of Hill coefficient in revealing the mechanistic details of protein–ligand binding and simultaneously, gives physical insight in the emergence of cooperativity from a microscopic viewpoint.

We have also determined the free energy change and its internal energy and entropy contributions, due to the protein–ligand binding based on the theory of stochastic thermodynamics. We have analytically shown that the free energy change due to the unrestricted non-cooperative binding mechanism is always more negative than the corresponding restricted binding mechanisms. Free energy change data for the tetrameric protein as a function of ligand concentration show that the binding is entropy driven at very low ligand concentration and gradually becomes energy driven with rise in ligand concentrations. This is true for the unrestricted non-cooperative binding scheme as well as for the restricted binding mechanisms, showing the absence of a general connection between binding efficiency and cooperativity. The model can be generalized further by imposing restrictions also on ligand detachment steps and taking any real number as the restriction parameter.

Acknowledgments K. Banerjee acknowledges the University Grants Commission (UGC), India for Dr. D. S. Kothari Fellowship.

References

1. D.L. Nelson, M.M. Cox, *Lehninger Principles of Biochemistry*, 4th edn. (Worth Publishers, New York, 2004)
2. T. Palmer, P. Bonner, *Enzymes: Biochemistry, Biotechnology, and Clinical Chemistry*, 2nd edn. (Horwood Publishing, West Sussex, 2007)
3. N. Bindslev, *Drug-Acceptor Interactions: Modeling Theoretical Tools to Test and Evaluate Experimental Equilibrium Effects*, 1st edn. (Co-Action Publishing, Sweden, 2008)
4. A.V. Hill, Physiol. J. **40**, 4 (1910)
5. J.J. Wyman, Protein Chem. Adv. **19**, 223 (1964)
6. B.E. Matthews, C.R. Biol. **328**, 549 (2005)
7. G.S. Adair, J. Biol. Chem. **63**, 529 (1925)
8. G. Weber, S.R. Anderson, Biochemistry **4**, 1942 (1965)
9. G.G. Hammes, C.W. Wu, Annu. Rev. Biophys. Bioeng. **3**, 1 (1974)
10. A. Goldbeter, Biophys. Chem. **4**, 159 (1976)
11. J. Ricard, A. Cornish-Bowden, Eur. J. Biochem. **166**, 255 (1987)
12. A. Conway, D.E. Koshland Jr., Biochemistry **7**, 4011 (1968)
13. A. Levitzki, D.E. Koshland Jr., Proc. Natl. Acad. Sci. USA **62**, 1121 (1969)
14. J. Monod, J. Wyman, J.P. Changeux, J. Mol. Biol. **12**, 88 (1965)
15. D.E. Koshland Jr., G. Nemethy, D. Filmer, Biochemistry **5**, 365 (1966)
16. H.P. Lu, L. Xun, X.S. Xie, Science **282**, 1877 (1998)
17. H.P. Lu, L. Xun, X.S. Xie, Science **282**, 1877 (1998)
18. S.C. Kou, B.J. Cherayil, W. Min, B.P. English, X.S. Xie, J. Phys. Chem. B **109**, 19068 (2005)
19. H. Qian, E.L. Elson, Biophys. Chem. **101**, 565 (2002)
20. P. Gaspard, J. Chem. Phys. **120**, 8898 (2004)
21. T. Schmiedl, T. Speck, U. Seifert, J. Stat. Phys. **128**, 77 (2007)
22. T. Schmiedl, U. Seifert, J. Chem. Phys. **126**, 044101 (2007)
23. W. Min, L. Jiang, J. Yu, S.C. Kou, H. Qian, X.S. Xie, Nano Lett. **5**, 2373 (2005)
24. H. Qian, Annu. Rev. Phys. Chem. **58**, 113 (2007)
25. D.T. Gillespie, J. Comput. Phys. **22**, 403 (1976)
26. D.T. Gillespie, J. Phys. Chem. **81**, 2340 (1977)
27. K. Banerjee, B. Das, G. Gangopadhyay, J. Chem. Phys. **136**, 154502 (2012)
28. D.T. Gillespie, Phys. A **188**, 404 (1992)
29. D.J. Evans, E.G.D. Cohen, G.P. Morriss, Phys. Rev. Lett. **71**, 2401 (1993)
30. G. Gallavotti, Phys. Rev. Lett. **77**, 4334 (1996)
31. C. Jarzynski, Phys. Rev. Lett. **78**, 2690 (1997)
32. D. Kondepudi, I. Prigogine, *Modern Thermodynamics: From Heat Engines to Dissipative Structures* (Wiley, Chichester, 1998)
33. J.L. Lebowitz, H. Spohn, J. Stat. Phys. **95**, 333 (1999)
34. G.E. Crooks, Phys. Rev. E **60**, 2721 (1999)
35. T. Hatano, S.I. Sasa, Phys. Rev. Lett. **86**, 3463 (2001)
36. E.M. Sevick, R. Prabhakar, S.R. Williams, D.J. Searles, Annu. Rev. Phys. Chem. **59**, 603 (2008). and references therein
37. C. Jarzynski, Annu. Rev. Condens. Matter Phys. **2**, 329 (2011). and references therein
38. U. Seifert, Phys. Rev. Lett. **95**, 040602 (2005)
39. V. Blickle, T. Speck, L. Helden, U. Seifert, C. Bechinger, Phys. Rev. Lett. **96**, 070603 (2006)
40. C. Tietz, S. Schuler, T. Speck, U. Seifert, J. Wrachtrup, Phys. Rev. Lett. **97**, 050602 (2006)
41. H. Abeliovich, Biophys. J. **89**, 76 (2005)
42. H. Ge, H. Qian, Phys. Rev. E **81**, 051133 (2010)
43. M. Esposito, C. Van den Broeck, Phys. Rev. E **82**, 011143 (2010)